Effects of Different Potential Models for the $^{16}O+^{144,154}Sm$ Fusion Reactions

Kyaw Thiha[1], Nyein Wint Lwin[2]

Abstract

Fusion cross sections are evaluated by numerically solving the Schrödinger equation within the following potentials under the incoming wave boundary conditions. Four versions of proximity potentials, three versions of Woods-Saxon parameterizations and a simple analytical fusion potential from the mean field description are employed. The fusion barrier heights and positions are also evaluated for asymmetry colliding systems. Coupled-channels calculations are also performed for $^{16}O+^{144,154}Sm$ systems. It is found that Prox 10, all versions of Woods-Saxon potentials and mean field potentials can reproduce the experimental barrier heights and barrier positions within ±5% for most of the colliding systems. The percentage deviations for other potentials vary up to ±14%. We can say that the largest deviation is found for the system, $^{40}Ca+^{124}Sn$ with largest charge product for most of the potentials. The comparison of fusion cross sections reveals that mean field potential reproduces the experimental data better than other potentials at energies above and below the Coulomb barrier.

Key words; Fusion cross section, nuclear potential, coulomb potential

Introduction

The cross section for the fusion of ^{16}O with the spherical and deformed isotopes at bombarding energies spanning the fusion barrier indicates the importance of nuclear deformation for the fusion process and depends sensitively on the shape of the colliding nuclei as well as the detailed properties of their low energies collective excitations. The large enhancement of the fusion cross section, and also the strong isotope dependence, are caused by the coupling of the relative motion between the projectile and target to their intrinsic degrees of freedom [Hagino, 1998]. For numerical calculations, Coupled-channels formulation is the preferred method. In the earlier period of the study of sub-barrier fusion, simplified coupled-channels codes such as CCFUS, CCDEF and CCMOD were

[1] Dr, Department of Physics, Lashio University
[2] Dr, Department of Physics, Mandalay University

widely used. Currently, newer codes are available to experimentalists and theorists, such as CCFULL[Hagino, 1999].

In heavy-ion fusion reactions involving a well-deformed nucleus, Rumin et al., has assumed that the orientation of the target nucleus does not change during the reaction. They have suggested the necessity of the couple–channels calculation beyond the orientation average formula for the systems with a large charge product of the projectile and target nuclei. Newton et al., compared the fusion barrier distributions obtained from the coupled-channels calculations with those obtained from experiments. He included coupling to all orders and treated excitation energies correctly.

Dasso et al., investigated the radial dependence of the nuclear potential at extremely close distances. Using the different versions of phenomenological proximity potential as well as other parameterizations within the proximity concept, Dutt et al., performed a comparative study of fusion barriers and cross sections using Wong formula but he did not take into account the couple-channels effect. On the other hand, Hagino et al., reported on the couple channels frameworks only with Woods-Saxon forms, though the various potentials have not been taken into account.

In order to fill a research gap in these studies, motivation of this work is to perform the fusion cross sections by using various inter-nuclear potentials and also take into account the channel-coupling effects.

In order to carry out detailed systematic studies of different fusion models, eight phenomenological potentials which will be used in this paper are described. These will be included four versions of proximity potentials [Dutt and Puri, 2010], three versions of Woods-Saxon parameterizations [Hagino, 1998] and a simple analytical fusion potential from the mean field description [Dobrowolski et al., 2003].

The Inter-Nucleus Potential Models

Firstly, we display the nuclear part of the interaction potential, V_N *(MeV)* as a function of inter-nuclear distance *r* (in femtometers) for the reaction $^{48}Ca+^{48}Ca$ using different phenomenological potentials in Fig. 1.a. For the clarity, only the prominent versions of these potentials are shown in this figure. We see that the AW 95 (BW 91) potentials follow the Woods-Saxon-type distributions. We see that the simple nuclear potential of mean field approaches show repulsive soft core at shorter distance but the

different versions of the proximity nuclear potentials have a repulsive hard core at shorter distance. We note that a repulsive core have appeared after approximating mean field potential as a Gaussian type, but original mean field potential may not have the repulsive core at small distance. In Prox 10 potential the counterbalance between the repulsive Coulomb and attractive nuclear part of the interaction potential occurs at larger distances, and hence it pushes the barrier outwards in Fig. 1.b.

In Fig. 2, we display the variation of surface energy coefficient γ with asymmetry parameter $A_s = \left[\frac{N_P+N_T-(Z_P+Z_T)}{N_P+N_T+(Z_P+Z_T)}\right]$. In this figure, we compare three versions of γ used in Prox 77, Prox 88, and Prox 00 potentials along with the relation suggested in AW 95 potential. For the present analysis, the mass of the reacting partner is kept fixed equal to $A_P = A_T = 48$ units. The surface energy coefficient depends strongly on the asymmetry of the reactions. A_s was increased by increasing the neutrons and decreasing the protons. For example, ${}^{48}_{24}Cr + {}^{48}_{24}Cr$ has $A_s = 0.0$. For $A_s = 0.42$, the reaction of ${}^{48}_{14}Si + {}^{48}_{14}Si$ whereas for $A_s = 0.25$, the reaction was ${}^{48}_{18}Ar + {}^{48}_{18}Ar$.

In all cases, the mass of the reacting partner is kept fixed, whereas the ratio A_s is varied by converting the proton into neutrons. At the end of this series, we have the reaction of ${}^{48}_{12}Mg + {}^{48}_{12}Mg$ having $A_s = 0.5$. From the figure, we see that the surface energy coefficient γ used in the latest proximity potentials Prox 00/Prox 10 as well as in original version Prox 77 is less sensitive toward the asymmetry of the colliding partners, whereas the one used in the Prox 88 potential has a stronger dependence on the asymmetry of the reacting nuclei. The coefficient γ of AW 95 yields same results like Prox 77. Since nuclear potential $V_N\ (r)$ depends directly on γ, one can conclude that the potentials calculated within Prox 00 and Prox 10 will be far less attractive for larger asymmetries compared to the one generated using Prox 77 and Prox 88. As a consequence, the potential pockets generated using Prox 00/10 are shallower than that calculated within Prox 88 (Prox 77).

In many studies, one finds that neutron excess, leads to more attraction. In these studies, the total mass of the colliding pair is not fixed and as a result, this dependence is more of mass dependence than of isospin dependence [Dutt and Puri, 2010].

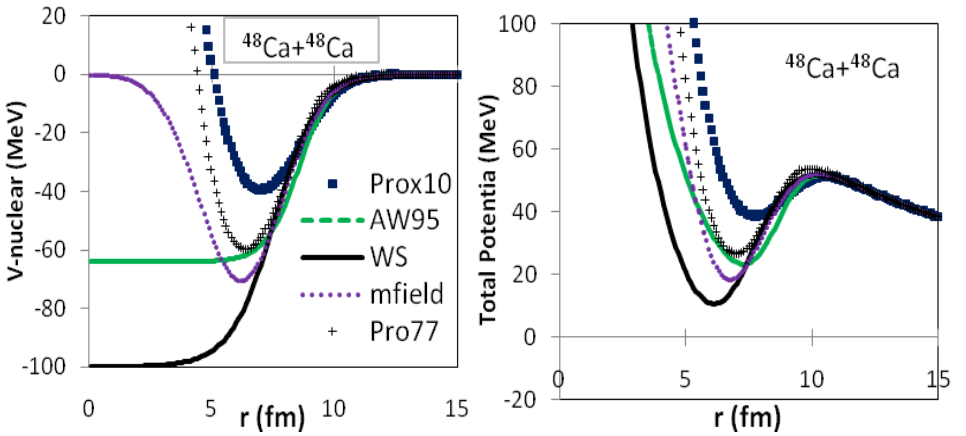

(a) **(b)**

Fig. 1. The nuclear part in Fig. (a) and the total in Fig. (b) of the interaction potential, V_N (MeV) as a function of internuclear distance r (in femtometers) for the reaction $^{48}Ca+^{48}Ca$ using different phenomenological potentials.

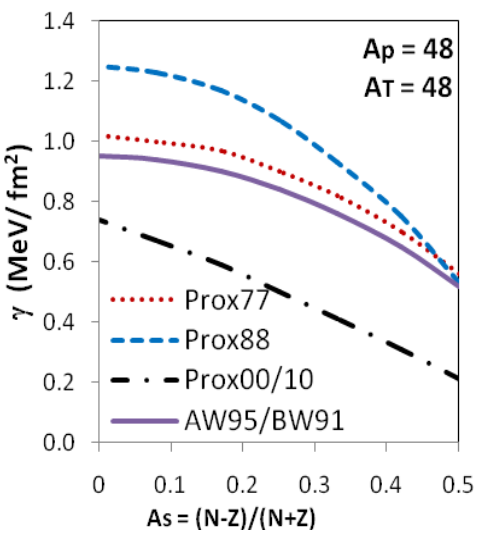

Fig. 2. The variation of the surface energy coefficient γ (MeV fm^{-2}) with asymmetry parameter A_s. We display the results using γ from Prox 77, Prox 88, Prox 00 and AW 95 for masses of reactions parameter A_P = A_T = 48 units.

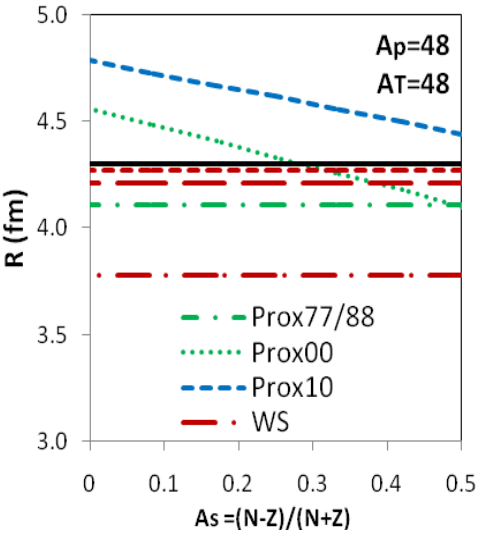

Fig. 3. The variation of radii used in the literature with asymmetry parameter A_s for masses of reactions parameter A_P = A_T = 48 units.

In Fig. 3, we display the dependence of different nuclear radii on the asymmetry parameter A_s. This parameter also plays significant role in nuclear potential and finally in the barrier calculations. We show the dependence of different forms of nuclear radii used in various potentials on the asymmetry parameter. We see that the radius used in the Prox 77 (also in Prox 88) and in all versions from Woods-Saxon parameterization (i.e., WS, BW 91 and AW 95) are independent of the asymmetry content, whereas, the one used in the Prox 10 (also in Prox 00) version depends on the asymmetry content of the colliding pairs. From Fig. 2 and 3 we see that both these parameters can lead to significant change in the nuclear potentials and ultimately in the fusion barriers even if the universal function $\Phi(\xi)$ is kept the same.

Results and Discussion

We calculate the percentage deviation ΔV_B (%) and ΔR_B (%) in Fig. 4, 5 and 6 as a function of asymmetry parameter A_s. The experimental values are taken from the Ref. [Dutt and Puri, 2010]. Using the simple analytical potential from the mean field description in Fig. 4, the fusion barrier heights are reproduced within $\pm$ 3.5% on average. On the other hand, this potential model reproduces fusion barrier positions within $\pm$ 5% for most of the colliding systems.

Interestingly, we see in Fig. 5 that Prox 00 fail to reproduce the barrier heights satisfactorily, whereas Prox 10 gives better results compared to other proximity potentials. We can report the discrepancy of the order of 4% between the results of Prox 77 (also Prox 88) and experimental data as was claimed in Ref. [Lin, 2004]. We note from Fig. 5 that Prox 10 potential reproduces the experimental fusion barrier heights within 3 %. In the previous sub-section, we mentioned that the interaction potential of Prox 10 occurs at larger distances than other proximity potentials. This behavior is clearly seen in the right panel of Fig. 5. Figure shows that Prox 10 gives larger barrier positions than all other proximity potentials.

From Fig. 6, it has been seen that the AW 95 (BW 91) potentials follow the Woods-Saxon-type distributions. The difference between the parameter sets used in AW 95 (BW 91) and Wood Saxon (WS) potential is that the sets of fixed parameters are used in AW 95 (BW 91) while that of free parameter are used in WS potential. Therefore, WS potential gets better results compared to other Woods-Saxon-type parameterizations (ie. AW 95 and BW 91).

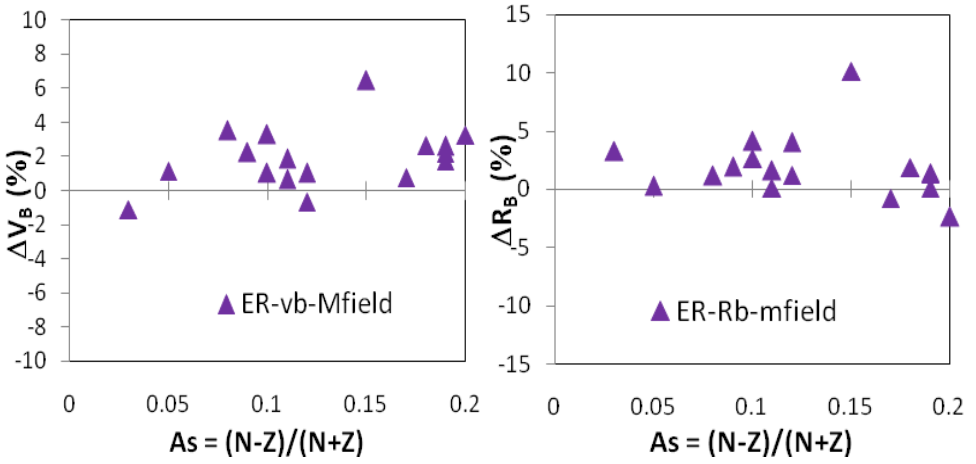

(a) (b)

Fig. 4. The percentage deviation ΔV_B (%) in (a) and ΔR_B (%) in (b) as a function of asymmetry parameter A_s using the simple analytical potential from the mean field description.

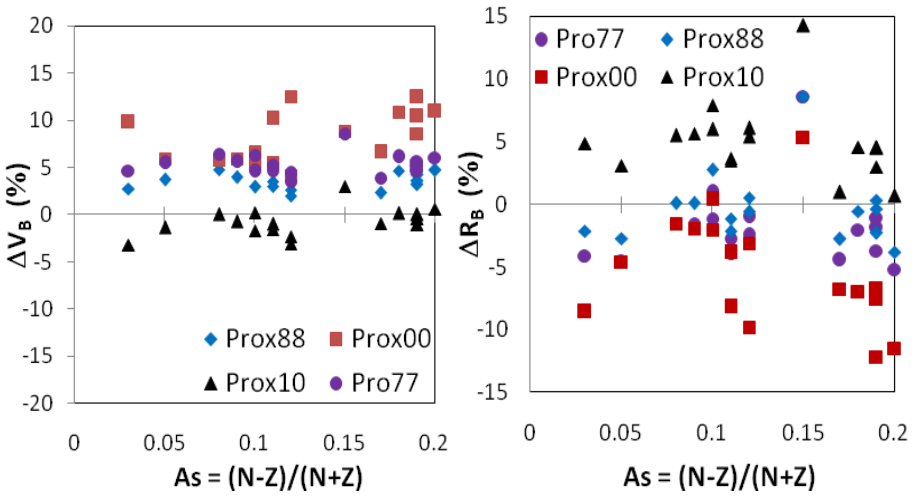

(a) (b)

Fig. 5. The percentage deviation ΔV_B (%) in Fig. (a) and ΔR_B (%) in Fig. (b) as a function of asymmetry parameter A_s using Prox 77, Prox 88, Prox 00 and Prox 10 potentials.

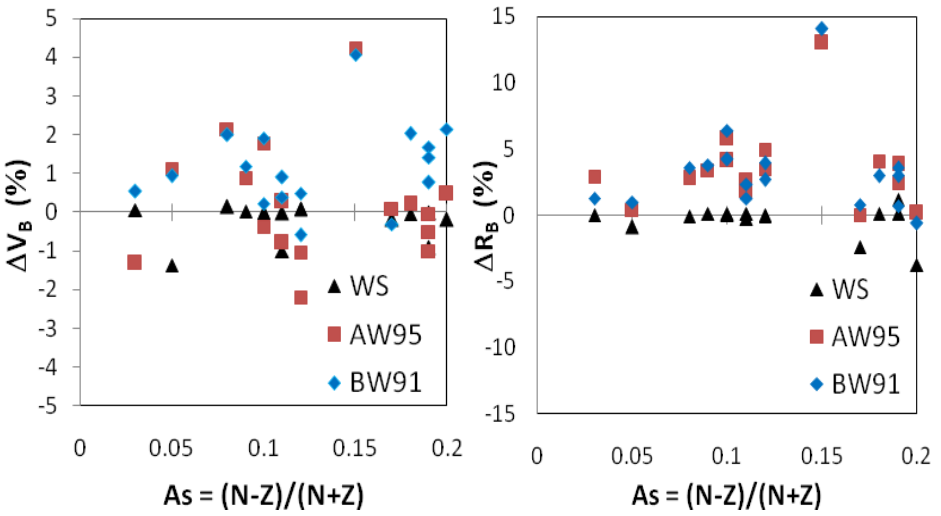

(a) (b)

Fig. 6. The percentage deviation ΔV_B (%) in Fig. (a) and ΔR_B (%) in Fig. (b) as a function of asymmetry parameter A_s using the WS, AW 95 and BW 91 potentials of the Wood-Saxon parameterization.

In summary, among eight phenomenological potentials, Prox 10, all versions of Woods-Saxon potentials and mean field potentials can reproduce the experimental barrier heights and barrier position within ±5% for most of the colliding systems. The percentage deviations for other potentials vary up to ±14%. It is noted from the calculated results that the largest deviation is found for the system, ^{40}Ca+^{124}Sn with largest charge product and asymmetry parameter $A_s \sim 0.15$.

Fig. 7 shows the experimental fusion excitation function for the $^{16}O+^{144}Sm$ and $^{16}O+^{154}Sm$ reactions and comparisons with the potential model. This Figure shows a comparison between the experimental fusion cross section and the exact fusion cross section by numerically solving the Schrödinger equation in the potential model. These are plotted as functions of the centre of mass energy for each reaction. We again observe that the experimental fusion cross sections drastically enhance compared with the predictions of the potential model. Moreover, we observe that the degree of enhancement of fusion cross section depends strongly on the target nucleus. The enhancement for the $^{16}O+^{154}Sm$ system is order of magnitude, while that for the $^{16}O+^{144}Sm$ system is about factor four at energies below the Coulomb barrier. These discrepancies were not due to the inadequate

behavior of the potential model for heavier systems, not because of the potential itself.

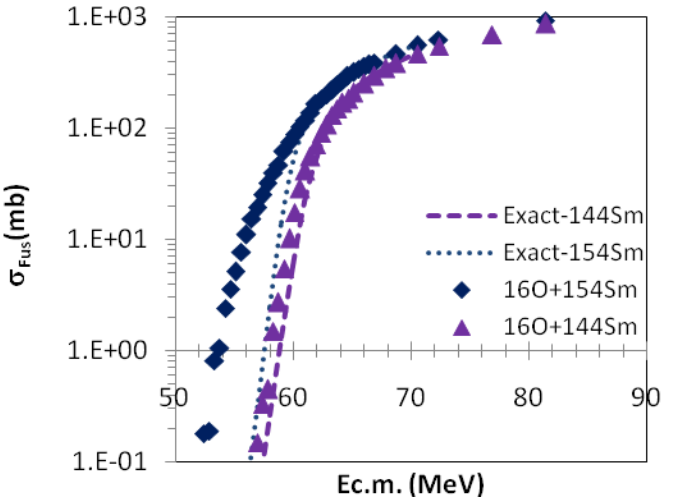

Fig. 7. The experimental fusion excitation functions for $^{16}O+^{154}Sm$ and $^{16}O+^{144}Sm$ reactions. This Fig. shows a comparison with exact numerical solutions.

We now calculate the fusion cross sections by numerically solving the Schrödinger equation. In Fig. 8 we display the fusion cross-sections $\sigma_{Fus}(mb)$ as a function of center-of-mass energy E_{cm} for the reactions of $^{16}O+^{144}Sm$ and $^{16}O+^{154}Sm$. The experimental values are taken from Ref. [Newton, et al., 2001]. As can be seen in the Fig. 8, the fusion cross sections at energies above the barrier are nicely explained by the mean field description and Woods-Saxon potential. But AW 95 (BW 91) as well as Prox 00 and Prox 88 fail to come closer to the experimental data. Mean field potential provides satisfactory results in both deformed and spherical systems, $^{16}O+^{154}Sm$ systems. This may be due to the fact that mean field description includes the microscopic information of the colliding systems. When we analyze the fusion cross section at energies below the barrier all of the parameterizations provide suitable results for spherical system $^{16}O+^{144}Sm$, ie., they give the same slopes as that of experimental data but not for deformed system. $^{16}O+^{154}Sm$. Prox 10 reproduces the fusion cross sections better than that of the mean field description. Inclusion of suitable coupling effects will improve the calculated results. In heavy-ion collision around the Coulomb barrier, the calculated results of fusion cross section

are sensitive to the values of the nucleus-nucleus potentials. So far, all nuclei considered are assumed to be spherical in nature; however, deformation as well as orientation of the nuclei (that is channel coupling) can affect the fusion cross section.

To study the effect of channel coupling using different potential types, we choose $^{16}O + ^{144}Sm$ and $^{16}O + ^{154}Sm$ reaction systems and perform channel-coupling calculations using CCFULL code. The authors of Ref. [Stokstad, et al., 1980] have shown that the coupled-channel effects, i.e. the vibrational coupling for this system is intimately related to the octupole vibration of ^{144}Sm, and that the quadrupole vibration plays only a minor role. Accordingly, we ignore the effects of the couplings to the quadrupole phonon states of ^{144}Sm and include only the single octupole phonon state at 1.81 *MeV*. The deformation parameter β_3 = 0.205 was used as in Ref. [Hagino, 1998]. The ion-ion potential was of a Woods-Saxon form. The depth, radius parameter and surface diffuseness were 105.1 *MeV*, 1.1 *fm* and 0.75 *fm* respectively, as given in Ref. [Hagino, 1998]. Because ^{144}Sm was a typical spherical nucleus the enhancement of experimental fusion cross section against the potential model is not evident. The next consideration is the $^{16}O + ^{154}Sm$ collision as a typical example of the rotational coupling. ^{154}Sm nucleus is a deformed prolate nucleus with quadrupole deformation of β_2= 0.3. But It was also found that the positive hexadecapole deformation (β_4 = +0.05) in ^{154}Sm is required in order to properly explain the experimental fusion cross sections.

The comparison of the calculated fusion cross sections are shown in Fig. 9 and 10. It is already mentioned that channel coupling effects greatly increased the calculated fusion cross section at energy below the Coulomb barrier. Thus, only the calculated cross sections for low energy regions are shown in the figures. As can be seen in these figures, proper coupling effects enhance the fusion cross sections and eventually match with the experimental data. Interestingly, we see that Prox 77/10 do not work well to reproduce the experimental data with vibrational coupling while the mean field potential cannot reproduce the experimental data with rotational coupling. It is observed that the agreement of Woods-Saxon-types is excellent in those degrees of freedom of target excitations.

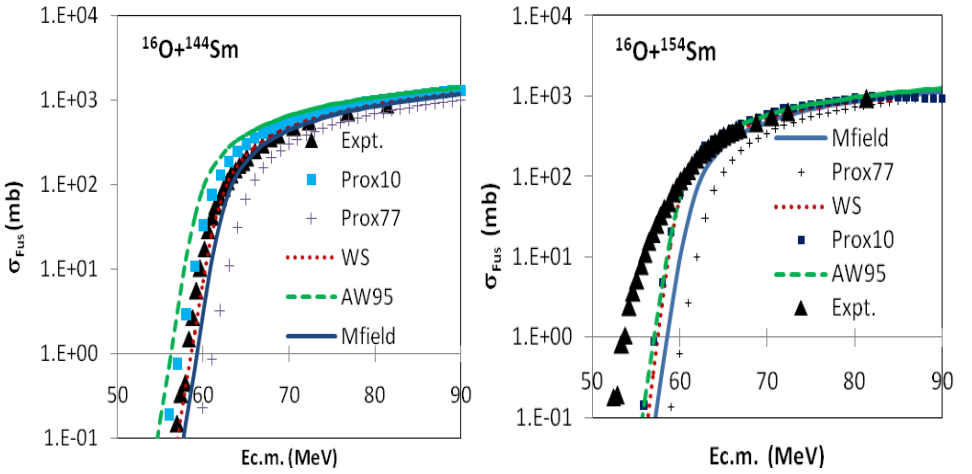

Fig. 8. The fusion cross sections obtained by numerically solving the Schrödinger equation for the reactions of $^{16}O+^{144}Sm$ (upper panel) and $^{16}O+^{154}Sm$ (lower panel) as a function of center-of-mass energy E_{cm}. in the logarithmic scale.

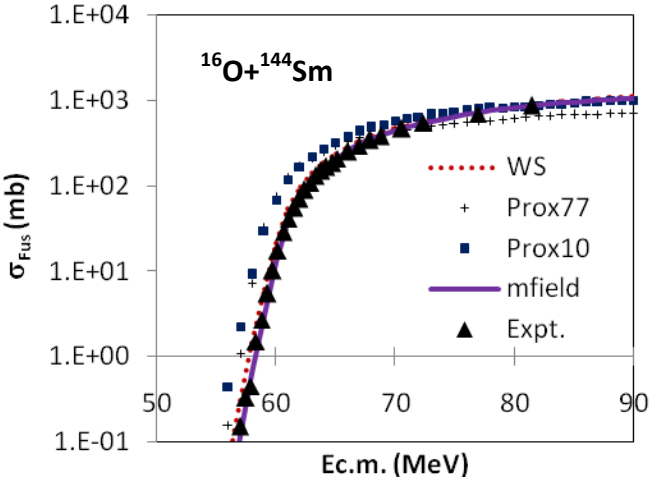

Fig. 9. Coupled-channels calculation of fusion cross sections for $^{16}O+^{144}Sm$ reaction including vibrational coupling effects.

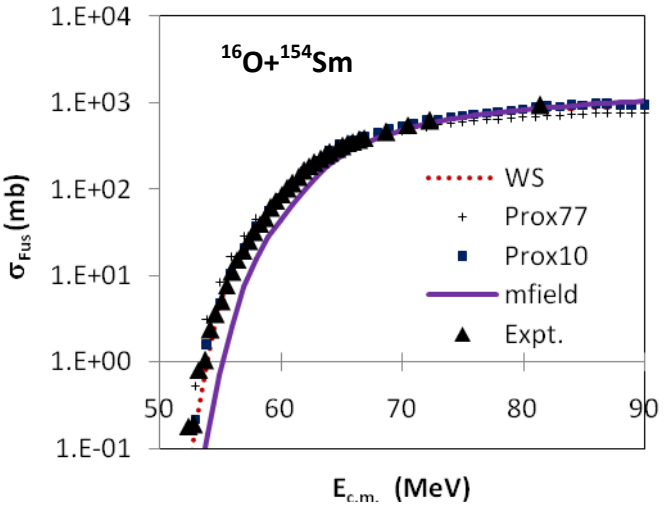

Fig. 10. Coupled-channels calculation of fusion cross sections for $^{16}O+^{154}Sm$ reaction including rotational coupling effects.

Conclusion

We have carried out a comparative study of heavy-ion fusion reactions using eight nuclear potential models. The dependence of the surface energy coefficients of nuclear potentials has been studied. Since nuclear potential V_N(r) depends directly on surface energy coefficient, one can conclude that the potentials calculated within Prox 00/10 will be less attractive for larger asymmetries compared to those generated by using Prox 77/88 and Woods-Saxon (WS) potentials. As a consequence, the potential pockets generated by using the former potentials are shallower than those obtained by using latter ones.

Fusion barriers for different potential models were extensively studied for asymmetric reactions. The experimental data were compared to various theoretical predictions. It was found that Prox 10, all versions of Woods-Saxon potentials and mean field potentials can reproduce the experimental barrier heights and barrier positions within ±5% for most of the colliding systems. The percentage deviations for other potentials vary up to ±14%. It has been found that the largest deviation is found for the system, $^{40}Ca+^{124}Sn$ with largest charge product for most of the potentials.

The comparison of fusion cross sections reveals that, in general, mean field potential reproduces the data better than other potentials at

energies above and below the Coulomb barrier. Woods-Saxon potential reproduces the comparable results with those of mean field potential but three free parameters are used in WS potential for each colliding systems. The calculated cross sections given by all nuclear potentials used in this work show the satisfactory results for spherical colliding systems but some deviations for deformed nuclei.

Acknowledgements

I would like to thank to Dr. Kay Thi Thin, Professor and Head of Department of Physics, Lashio University for her permission to write this research paper. My deepest gratitude is extended to my collaborator, Kouhei Washiyama, RIKEN in Japan for providing me the research topic I really enjoyed and for the learning process.

References

Hagino, K. (1998) "PhD. Thesis", Tohoku University.

Hagino, K. et al., (1999) Comp. Phys. Lett. **123**, 145.

Rumin, T. et al., (2001) Phys. Rev. **C 63**, 044603.

Newton, J. O. et al., (2001) Phys. Rev. Lett. **C 64**, 064608.

Dasso, C.H. and Pollaralo, G. (2003) Phys. Rev. **C 68**, 054604.

Dutt, I. and Puri, R. K. (2010) Phys. Rev. **C 81**, 064608.

Dobrowolski, A. et al., (2003) Nucl. Phys. **A 729**, 713.

Dutt, I. and Puri, R. K. (2010) arXiv:nucl-th **2**, 1005.5213.

Lin, C.J. (2004) Prog. Theor. Phys. **154**, 184.

Stokstad, R.G. et al., (1980) Phys. Rev. Lett. **C 21**, 2427.